Articles

High-Throughput Screening Using Porous Photoelectrode for the Development of Visible-Light-Responsive Semiconductors

Takeo Arai,[†] Yoshinari Konishi,[†] Yasukazu Iwasaki,[‡] Hideki Sugihara,[†] and Kazuhiro Sayama*,[†]

Energy Technology Research Institute, National Institute of Advanced Industrial Science and Technology (AIST), Central 5, 1-1-1 Higashi, Tsukuba, Ibaraki 305-8565, Japan, and Nissan Research Center, Nissan Motor Co., Ltd., 1 Natsushima, Yokosuka, Kanagawa 237-8523, Japan

Received January 18, 2007

A high-throughput screening system for new visible-light-responsive semiconductors for photoelectrodes and photocatalysts was developed in this study. Photoelectrochemical measurement was selected to evaluate visible-light responsiveness, and an automated semiconductor synthesis system that can be used to prepare porous thin-film photoelectrodes of various materials was also developed. As an example application of our system, iron-based binary oxides were selected as target materials for n-type semiconductors. Fe−Ti, Fe−Nb, and Fe−V with various composition ratios were synthesized. Fe−Ti and Fe−Nb binary oxide systems have been studied previously, and our results showed good consistency with previous reports, demonstrating the capability of our system. In the Fe−V system, the highest photocurrent was observed with 50% vanadium. This ratio corresponds to $FeVO_4$, which is expected to be a new visible-light-responsive material. As another example, screening targets of bismuth-based binary oxides were investigated for p-type semiconductor photoelectrodes, and $CuBi_2O_4$ was found as a new visible-light-responsive p-type semiconductor.

1. Introduction

Ever since Fujishima and Honda reported on the use of TiO_2 photoelectrodes for water splitting under UV-light irradiation,[1] it has been expected that photoelectrodes and photocatalysts would emerge as important technologies for energy production and environmental purification using sunlight. TiO_2 that work under UV light are currently in practical use as photocatalysts for environmental purification.[2] Although much effort has been devoted to the development of visible-light-responsive semiconductors for photocatalysts,[3−6] no efficient semiconductor has been found to be of practical use under visible light. In the field of photoelectrode development, nanocrystalline semiconductor thin films with porous structure such as WO_3, Fe_2O_3, and $BiVO_4$ on conducting glass electrodes have shown excellent incident photon-to-current conversion efficiencies (IPCE) for water decomposition under visible light,[7−12] compared with single-crystal- or pellet-type photoelectrodes. However, the solar energy conversion efficiencies were not sufficient for practical use with regard to charge separation, light absorption, photocurrent−potential dependence, the energy levels of the conduction and valence bands, and stability. To utilize solar light effectively, new semiconductors that work under visible light with high efficiency in photoelectrodes and photocatalysts must be developed.

However, it is difficult to say that the search for new semiconductor materials has proceeded expeditiously. In the screening of semiconductor materials, there are more than 1000 patterns of combinations of ordinary elements even in the case of a binary oxide. The number of target materials is enormous for mixed oxides that consist of more than three metals with various composition ratios; therefore, a manual search of such materials is difficult. Therefore, to accelerate the screening of semiconductor materials, their synthesis and evaluation should be speedy, easy, and automatic. We developed a high-throughput screening system for new visible-light-responsive semiconductors for photoelectrodes and photocatalysts. We selected photoelectrochemical measurement to evaluate the charge separation ability of visible-light-responsive semiconductors, and we developed an automated synthesis system for photoelectrode library (array of samples) using the metal organic decomposition (MOD) method and evaluation system for screening.

As an example application of our system, iron-based binary oxides, known as n-type semiconductor photoelectrodes, were selected as target materials. Iron-based binary oxide systems such as Fe−Ti, Fe−Nb, and Fe−V were synthesized with various composition ratios, and their photocurrents were evaluated. In another example, screening targets of bismuth-

* To whom correspondence should be addressed. E-mail: k.sayama@aist.go.jp.

[†] National Institute of Advanced Industrial Science and Technology (AIST).

[‡] Nissan Motor Co., Ltd.

10.1021/cc0700142 CCC: $37.00
Published on Web 06/16/2007

based binary oxides were investigated for p-type semiconductor photoelectrodes.

2. Experimental Section

2.1. Features and Advantages of Our Screening System. We selected photoelectrochemical measurement for speedy and easy evaluation of the charge separation ability of visible-light-responsive semiconductors. In this measurement, photoexcited electrons and holes are forced to separate by application of a potential, and then they are detected as photocurrent. It is sufficient to evaluate the properties of photoexcitation and charge separation simply by visible light. In the process of screening for photocatalysts,[13,14] evaluation of the photocatalytic activity of semiconductors is difficult and time-consuming because photocatalytic activity depends strongly on measurement conditions, the type of substance, cocatalysts, etc. Therefore, if the visible-light responsiveness of a material could be confirmed by photoelectrochemical measurement before the evaluation of photocatalytic activity, the screening process would be more efficient. Furthermore, the type of semiconductor (n- or p-type) could also be confirmed by checking the photocurrent properties of the targeted material. There have been reports regarding the enhancement of photocatalytic activity by heterojunctions of semiconductors[15−17] and the photoelectrolysis of water by heterojunction photoelectrodes[18,19] or a combination of p- and n-type photoelectrodes.[20−22] It is expected that new photoelectrodes and photocatalysts will be developed by using the n- and p-type semiconductors found by the screening system.

There have been reports on the screening of photoelectrodes, and features of the synthesis and evaluation methods are mentioned below. McFarland et al. synthesized semiconductor films on conductive glass substrates by electrochemical deposition and evaluated their photocurrent properties using a special electrochemical probe.[23] However, in photoelectrode synthesis by electrochemical deposition, semiconductors that can be synthesized electrochemically are limited, and the preparation of mixed-metal semiconductors is difficult because the speed of electrodeposition from a solution containing various metal ions is different according to the elements. Parkinson et al. used ink-jet printing to prepare photoelectrodes.[24] They printed overlapping patterns of soluble metal nitrate salts, as metal oxide precursors, onto a conductive glass substrate, fired it to obtain metal oxides, and measured the photocurrent. The resulting photocurrent from the photoelectrochemical cell was recorded as mapping data. A preparation method using a wet process is highly versatile, but in the case of ink-jet printing, solutions are printed on the substrate individually, and it is not precisely known whether the solutions are mixed at the molecular level on the substrate. Many mixed oxides consist of an integer ratio of metals, but there is uncertainty about the correctness of the metal ratio and about contamination.

To solve these problems, we selected the MOD method using organic solvents, and the solutions were mixed using an automated liquid-handling platform before printing and firing. In the MOD method, metal ions are dispersed at the atomic level and stabilized by organic compounds, and there is less concern about precipitation after mixing of the solutions than there is with a method using an aqueous solution. Furthermore, this method is useful for the preparation of porous films because the organic solvent or additives (viscosity-improver) in the preparation solution control the porous structure during the calcination process. Porous thin-film photoelectrodes have the advantage that the diffusion length of the electrons or holes formed by the band gap photoexcitation is significantly shorter than that with conventional thick photoelectrodes. Because the electrolyte solution can penetrate into pores over the whole nanocrystalline semiconductor film, electrons or holes in the nanoparticle can move quickly to the semiconductor-electrolyte interface. In the preparation process, the solutions were mixed at the molecular level to exact ratios using an automated liquid-handling platform. The mixed solutions were printed on conductive glass substrates and fired. Disposable tips were used in the mixing and printing process to prevent contamination. A similar preparation method was used in the screening of the thermoelectric elements,[25] but the quality of the film was not good enough for photoelectrodes; therefore, we used the following special technique to prepare high-quality photoelectrodes.

The photocurrent is affected by the contact between semiconductor particles or the semiconductor and conductive substrate. In the preparation of photoelectrode films with sufficient thickness for light absorption, when highly concentrated solutions are used or a large amount of solution is printed on the substrate at the same time, a thick film with many cracks will be synthesized, and this film will easily exfoliate from the substrate. The main reason for the cracks and exfoliation of the film is self-shrinkage during calcination. Therefore, it is particularly important to overprint very thin films layer by layer, that is, to overprint low-concentration MOD solutions on the substrate. A porous structure with flexibility and the technique of overprinting very thin films repeatedly layer by layer can release the tension of self-shrinkage, resulting in high-quality film with a high photocurrent. To make high-quality film automatically, we combined an automated liquid-handling platform to print the samples and a robot arm with highly accurate mobility to transfer them between the automated liquid-handling platform and an electric furnace. This combination made it possible to print the solution at the same position and fire it several times automatically. This system makes it easy to check the dependence of photocurrent on film thickness.

In our system, there are two procedures for evaluation of the visible-light response of the semiconductor: the high-speed evaluation procedure (HEP) and the detailed evaluation procedure (DEP). The features of the two procedures are compared in Table 1. HEP is performed using a photoelectrode in which several samples are printed on one substrate, in the same way that was reported by Parkinson et al.[24] The photoelectrode is immersed in electrolyte, and every sample on the substrate is scanned with focused light. This method has the advantage that the photocurrents of many samples can be evaluated quickly and convenient, it is suitable for brief screening of visible light responsiveness. But the method has the disadvantages that one sample could affect other samples on the same substrate and that a sample to

Table 1. Comparison between HEP and DEP

	HEP	DEP
purpose	brief and speedy evalutation	detailed evaluation
no. of samples on one substrate	42 samples (max)	1 sample
photoelectro-chemical evaluation	photocurrent at fixed potential	current−potential current−time IPCE
other evaluations	difficult	XRD, XRF, SEM, etc.
advantage	speedy and convenient	free from the effects of other samples
disadvantage	effects of other samples	duration

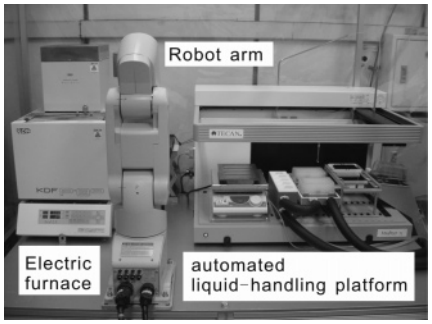

Figure 1. Automated semiconductor synthesis system.

which potential is applied for a long time could change during the measurement. To solve these problems, we synthesized and evaluated the semiconductor films individually, with the DEP. In this method, various photoelectrochemical measurements such as current−potential measurement, current−time measurement, and incident photon-to-current conversion efficiencies are available. Furthermore, the samples could be characterized using XRD, XRF, SEM, etc. But it takes a long time to evaluate photocurrent property of many samples compared with the HEP. We tried to make the screening process efficient for an enormous number of samples by using both of these procedures. The screening scheme of this system is as follows. First, materials are synthesized and evaluated by HEP, and samples that show high visible-light responsiveness are selected briefly and quickly. Selected samples are synthesized individually to confirm their photocurrent properties and to identify the material using the DEP.

Details about the automated semiconductor synthesis system and the effective evaluation system are described below.

2.2. Automated Semiconductor Synthesis System. The automated semiconductor synthesis system developed in this study is shown in Figure 1. This system consists of an automated liquid-handling platform (Tecan Japan, Mini-Prep75) for mixing and printing the solution, an automated electric furnace (Denken, KDF P-80, max 1100 °C) for firing samples up to 900 °C, and a robot arm (Mitsubishi Electric, RV-1A) for transferring the samples between the automated liquid-handling platform and the electric furnace. In the automated liquid-handling platform, there are 5 containers for large amounts of precursor solutions (max 25 mL) and 96 containers for small amounts (max 1 mL) to handle

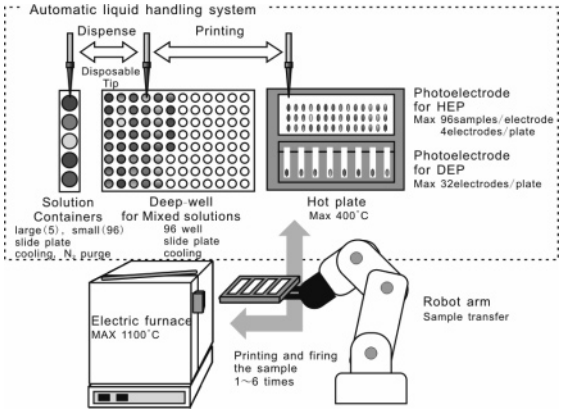

Figure 2. Scheme of photoelectrode synthesis.

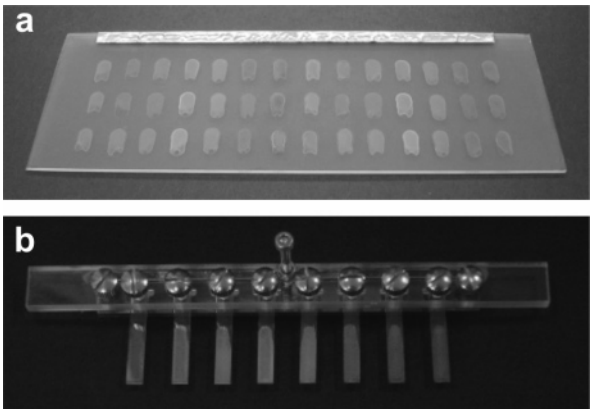

Figure 3. Photograph of the photoelectrode for high-speed evaluation (a) and photoelectrodes for detailed evaluation (b).

several different metal ions at the same time, and various oxides such as complex materials and doping materials can be prepared. Various solutions, including aqueous solutions, are available as precursor solutions. The precursor solutions in containers are dispensed into a deep well and mixed well by repeated aspiration and dispensing using a disposable tip. The disposable tip is replaced for every solution to prevent contamination. Solution containers and the deep well for sample preparation are cooled with circulating water and capped with an automated slide plate to prevent evaporation of the solution, and they are purged with dry N_2 gas to keep out oxygen and moisture from the air to avoid alteration of the precursor solution. In the printing process, a small amount of sample solution is dispensed on the conducting glass substrate and is spread by trailing the head of the disposable tip. Excess solution on the substrate is removed by aspiration to make a thin solution layer. The evaporation speed and spreading of the solution can be also controlled by adjusting the temperature of the substrate (Figure 2).

This system can synthesize the 2 patterns of photoelectrode for HEP and DEP. For the HEP, various samples are synthesized on the same conductive glass substrate (114 mm × 40 mm), as shown in Figure 3(a). There are 42 samples per substrate in the standard condition and four substrates available in one experiment. This means 168 samples can be synthesized in a day in just one experiment, yielding over 60 000 synthesized samples in a year. On the other hand, in the DEP, the semiconductor films are synthesized individu-

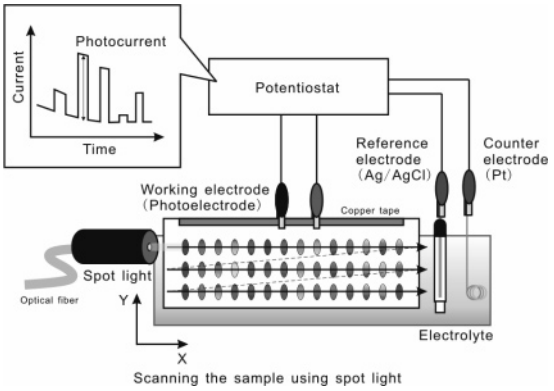

Figure 4. High-speed evaluation procedure. The photocurrent of a sample is evaluated by scanning the photoelectrode with focused light while applying a constant potential. The potential was set to 1.0 and −0.1 V (vs. Ag/AgCl) for the screening of n- and p-type semiconductors, respectively.

ally on small conductive glass substrates (5 mm × 30 mm) (Figure 3b). One experiment can synthesize 32 samples.

2.3. Evaluation Scheme of Synthesized Photoelectrodes. For HEP, the photocurrent of a sample is evaluated by scanning the photoelectrode synthesized for HEP (Figure 3a) with focused light, while a constant potential is applied (Figure 4). The size of the glass substrate was decided by consideration of the effect of glass conductivity. The photocurrent measurement was performed using a potentiostat (Toho Giken, PS-08) and a Pyrex glass cell. Sodium sulfate aqueous solution (0.1 M, pH 5.8) or sodium dihydrogen phosphate aqueous solution (0.1 M, adjusted to pH 7.0 with sodium hydroxide) was used as an electrolyte. Copper foil was taped on the top of the photoelectrode to connect the cables for the working electrode (Figure 3a). An Ag/AgCl electrode and a platinum wire were used as the reference and counter electrodes, respectively. A xenon lamp (Perkin-Elmer, CERMAX 300W) equipped with an optical fiber and a 420 nm cutoff filter (HOYA, L-42) was used as the light source. The edge of the optical fiber was covered with a 1-mm hole slit and fixed on the XY stage to scan light on the sample. The photocurrent was evaluated by measurement of the current difference between when the light on the sample was turned on and off while applying a constant potential. The potential was set to 1.0 and −0.1 V (vs Ag/AgCl) for the screening of n- and p-type semiconductors, respectively.

On the other hand, in the DEP, synthesized samples for DEP (Figure 3b) are individually evaluated for their photocurrent properties by current−potential measurement and current−time measurement. From the results, information about the open circuit potential, dark current and photocurrent properties, and stability can be obtained. The photoelectrodes can also be used to identify the crystal phase, the composition ratio, the morphology of particles, etc. Current−potential measurement was performed using a potentiostat (BAS, Als660s) and a Pyrex glass cell. A xenon lamp (Ushio Denki, 500W) was used as light source. The photoelectrode was masked with a 2-mm hole slit and was irradiated with chopping light. A 0.1 M sodium sulfate aqueous solution was used as an electrolyte. An Ag/AgCl electrode and a platinum wire were used as reference and counter electrodes, respectively. Material identification was performed using an X-ray diffractometer (XRD, Bruker AXS, MX-Labo). The morphology observation of the film was performed using a scanning electron microscope (SEM, Hitachi, S-800).

Moreover, some methods to reduce the effect of the inhomogeneity of the film thickness on the photocurrent were used in both HEP and DEP as follows. The photocurrent is generally sensitive with the inhomogeneity of the film thickness when the average film thickness is very thin. Therefore, we over-painted the film 4 times as a standard condition. The photocurrent was measured by irradiating light from the conductive glass side to shorten the diffusion length of electron and holes. Furthermore, it was measured in 4 different points at one sample area and the maximum value was selected as the photocurrent of sample.

2.4. Application to Visible-Light-Responsive Semiconductor Screening using Our System. We used our system to screen for visible-light-responsive semiconductors. First, we controlled the printing conditions to make homogeneous films. Homogeneity of the film is required for the photocurrent measurement. In addition, in the HEP, many samples are printed on the same glass substrate to evaluate the photocurrent quickly, so preventing contact between samples is important. In this study, the printing condition was controlled by the temperature of the substrate and by the addition of a viscosity-improver solution to the precursor solution. The spread of the solution could be controlled by the temperature of the substrate by acceleration of the evaporation of solution. The viscosity-improver solution was added to control the spread of the sample and to prepare a homogeneous film. Ethyl cellulose was selected as the viscosity-improver because it shows a high affinity with the EMOD solutions used in this study. The solution was prepared by dissolution of ethyl cellulose in butyl acetate as a solvent at 10 wt %.

Fluorine-doped tin oxide (FTO) conductive glass provided by Asahi Glass Co. and an enhanced metal organic decomposition (EMOD) solution of bismuth provided by Symmetrix Corporation, diluted to 0.2 M with butyl acetate, were used as the substrate and precursor solutions, respectively. The dependence of the printed sample condition on the substrate temperature was examined by changing the temperature of the glass substrate from 30 to 150 °C. Second, the viscosity-improver solution was added to the MOD solution, and the amount was changed from 0 to 90 vol % to control the printing condition.

After optimization of the printing condition, the sample was prepared by mixing MOD and viscosity-improver solutions using the automated liquid-handling platform and printing on an FTO substrate. For the screening of n-type semiconductor photoelectrodes targeted at iron-based binary oxides, an MOD solution of each metal diluted at 0.2 M with butyl acetate was used, and the mixing ratio of the two metals was changed from 0 to 100 mol % with a 5 mol % step size. For the screening of p-type semiconductor photoelectrodes targeted at bismuth-based binary oxide, materials with confirmed crystal structures were selected as target materials, and samples were prepared by mixing the MOD solution of desired metal with that of bismuth at the desired composition ratios. In this experiment, the MOD solution

Figure 5. Effect of temperature on printing condition. The bismuth solution was printed on the conductive glass substrate at various temperatures.

Figure 6. Effect of viscosity-improver on printing condition. The bismuth solution was mixed with viscosity-improver at various ratios. The viscosity improver was prepared by dissolution of ethyl cellulose in butyl acetate as a solvent at 10 wt %.

was used without dilution. The printed samples were transferred into the furnace by the robot arm and fired at 550 °C for 30 min in air. For the high-temperature treatment condition, the synthesized samples were fired at 700 °C for 30 min in air. The synthesized photoelectrodes were evaluated for their photoelectrochemical properties using the HEP and DEP as explained above.

3. Results and Discussion

3.1. Control of Printing Condition. The printing condition was optimized for the preparation of high-quality films for several metal solutions by changing the temperature of the substrate and the amount of viscosity-improver added to the MOD solutions. The case of bismuth is shown as an example in Figure 5. The spread area of the solution was decreased by increasing the temperature. The solution spread widely at less than 50 °C; therefore, the film area could not be controlled. On the other hand, the shape of the film area could be controlled at temperatures from 70 to 110 °C. At over 130 °C, the spread area was very small, and the film became inhomogeneous. The best homogeneous film was obtained around 70 °C, so the substrate temperature was adjusted to be approximately 70 °C.

Next, the optimal amount of viscosity-improver added to the solution was examined (Figure 6). The spread of the solution was reduced, and the area of the sample became smaller with an increased amount of viscosity-improver. By comparison of films with and without viscosity-improver, we confirmed that the film area could be controlled and that the apparent homogeneity of the film thickness could be improved by addition of the viscosity-improver. However, when an excess of viscosity-improver was added to the solution, the sample became inhomogeneous and easy to detach from the substrate. Thus, the amount of viscosity-improver added to the solution was adjusted to be 50−75 vol % (standard 75 vol %). Almost all films prepared from various MOD solutions under optimized temperature and viscosity were homogeneous, so we selected these as the basic preparation conditions. The reproducibility of the samples was evaluated by photocurrent measurement using TiO_2 film. TiO_2 was suitable to evaluate the reproducibility by photocurrent because of its stability. Forty-two samples

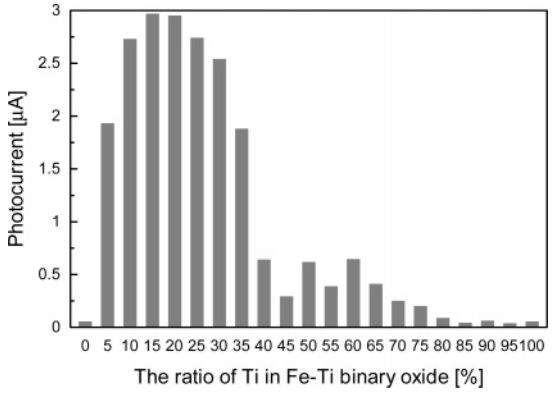

Figure 7. Dependence of photocurrent on the Ti ratio in Fe−Ti binary oxides (HEP). The photoelectrode was prepared by painting and firing at 550 °C for 30 min, four times, using HEP. It was finally fired at 700 °C for 30 min. Electrolyte: 0.1 M NaH_2PO_4 aqueous solution (pH 7.0). Applied potential: 1.0 V (vs Ag/AgCl). Light source: Xe lamp with 420 nm cutoff filter (3.2 mW).

of TiO_2 film were prepared using HEP in the condition mentioned above, and the standard variation of photocurrent was about 3% to the average value.[26]

3.2. Screening for n-Type Semiconductors in Various Iron-Based Binary Oxides. We selected iron-based binary oxides as a target material because there have been reports on the photoelectrochemical properties of various iron-based binary oxides,[10,12] and these results can be compared with our results to check the reliability of our system. We examined the photocurrent properties of various combinations of Fe−M (M = Si, Ca, Ti, V, Cr, Zn, Zr, Nb, In, Sn, Bi)[27] with various composition ratios. In some combinations, we observed higher photocurrents than with pure iron oxide. Here, we select the Fe−Ti, Fe−Nb, and Fe−V systems as examples. In the Fe−Ti system, an improvement of photocurrent compared with pure Fe_2O_3 was observed from 5% Ti synthesized in the HEP at 700 °C, and a sample with 20% Ti showed the highest photocurrent (Figure 7). An Fe_2O_3 photoelectrode doped with Ti has been reported by Augstynski et al.[10] In their study, Fe_2O_3 doped with 5% Ti showed a higher photocurrent than undoped Fe_2O_3. Our results correspond well with theirs. A sample with 5% Ti prepared in the DEP showed a pattern only of Fe_2O_3 (hematite) in an XRD measurement, and it was suggested that Ti was doped in Fe_2O_3. In the Fe−Nb system, a sample with 15% Nb synthesized in the HEP at 700 °C showed the highest photocurrent (Figure 8). Miyake and Kozuka have reported on Fe_2O_3−Nb_2O_5 film.[12] They observed the highest photocurrent at Nb/(Fe + Nb) = 0.25, among Nb/(Fe + Nb) = 0.0, 0.25, 0.75, and 1.0. In our study, the sample with 25% Nb showed the highest photocurrent among Nb ratios of 0, 25, 50, 75, and 100%. These results correspond well with previous reports by Miyake and Kozuka. This consistency is a good example of the capability of our system. For the Fe−V system, a sample with 50% V synthesized in the HEP at 550 °C showed the highest photocurrent (Figure 9). In the DEP, the XRD pattern of the photoelectrode with 50% V was too broad and noisy to identify the compound of the oxide semiconductor because of the thinness of the film (<1 μm) and its low crystallinity. However, we confirmed that the powder synthesized using a large amount of the precursor

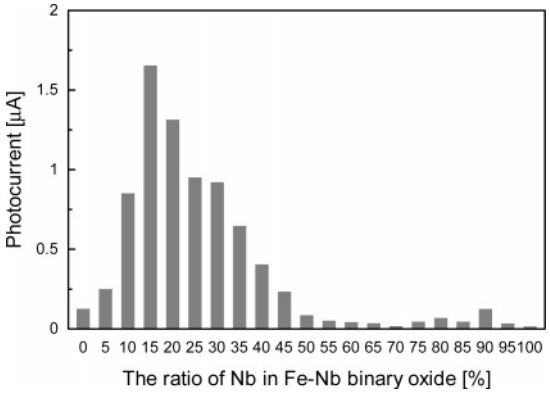

Figure 8. Dependence of photocurrent on the Nb ratio in Fe−Nb binary oxides (HEP). The photoelectrode was prepared by painting and firing at 550 °C for 30 min, four times, using HEP, and it was finally fired at 700 °C for 30 min. Electrolyte: 0.1 M NaH_2PO_4 aqueous solution (pH 7.0). Applied potential: 1.0 V (vs Ag/AgCl). Light source: Xe lamp with 420 nm cutoff filter (3.2 mW).

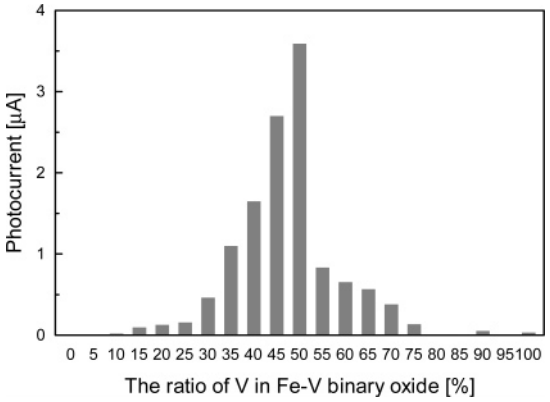

Figure 9. Dependence of photocurrent on the V ratio in Fe−V binary oxides (HEP). The photoelectrode was prepared by painting and firing at 550 °C for 30 min, four times, using HEP. Electrolyte: 0.1 M NaH_2PO_4 aqueous solution (pH 7.0). Applied potential: 1.0 V (vs Ag/AgCl). Light source: Xe lamp with 420 nm cutoff filter (3.2 mW).

solution at 550 °C showed mainly the XRD pattern of $FeVO_4$. We therefore inferred that mainly very fine $FeVO_4$ with low crystallinity was synthesized in the photoelectrode. A porous structure was confirmed by SEM observation. The $FeVO_4$ particles were 20−30 nm in diameter. The color of the sample with 50% V was brownish yellow, and the threshold of the absorption spectrum was approximately 600 nm. Furthermore, the passage of photoelectrons (Coulomb number) for 1 h was about 0.013 C (0.13 μmol), whereas the amount of $FeVO_4$ under irradiation was approximately 0.07 μmol. Therefore, from the result of the current−time measurement, the turnover number of the observed photoelectrons to the $FeVO_4$ unit was greater than 1. After the measurement, there was no change in the appearance of the $FeVO_4$ film. This material is expected to be a new promising n-type semiconductor with high efficiency under visible light.

3.3. Screening for p-Type Semiconductors in Bismuth-Based Binary Oxides. For bismuth-based mixed-oxide semiconductors, it is inferred that the valence band (VB) was shifted because of the Bi-6s orbital, and several compounds, such as $BiVO_4$,[6,8] $Bi_2W_2O_9$,[28] $CaBi_2O_4$,[29] $BiTa_{0.8}Nb_{0.2}O_4$,[30] and $PbBi_2Nb_2O_9$,[31] have been reported to be efficient photocatalysts and photoelectrodes. The screening

Table 2. Bismuth-Based Binary Oxides Selected from XRD Data Marked as Highly Reliable

	1	2	3
1	$ZnBi_{38}O_{60}$	$Bi_{7.65}Zn_{0.35}O_{11.83}$	$SrBiO_3$
2	$Sr_3Bi_2O_6$	$SrBi_2O_4$	$CuBi_2O_4$
3	$Ca_4Bi_6O_{13}$	$Ca_2Bi_2O_5$	$Bi_{48}Al_2O_{95}$
4	$Al_4Bi_2O_9$	$Bi_{0.67}Y_{0.33}O_{1.5}$	$Y_{0.285}Bi_{0.715}O_{1.5}$
5	$Bi_{1.87}Y_{0.13}O_3$	$Bi_{12}NiO_{19}$	$Bi_{3.64}Ni_{0.36}O_{5.82}$
6	$Bi_{3.69}Mn_{0.31}O_{6.15}$	$Bi_2Fe_4O_9$	$Bi_{25}FeO_{40}$
7	$Bi_{24}Fe_2O_{39}$	$Bi_{12}MgO_{19}$	Blank

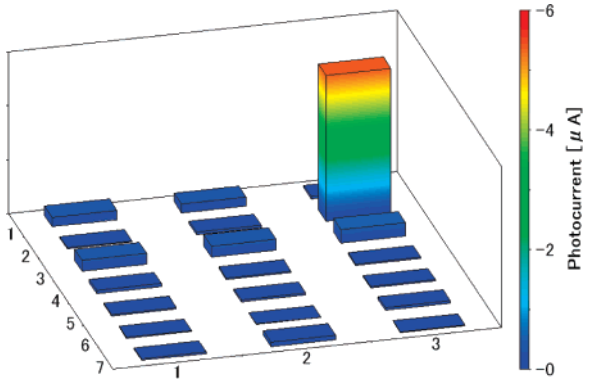

Figure 10. Photocurrent mapping of various bismuth-based binary oxides. The photoelectrode was prepared by painting and firing at 550 °C for 30 min, one time, using HEP. Electrolyte: 0.1 M Na_2SO_4 aqueous solution (pH 5.8). Applied potential: −0.1 V (vs Ag/AgCl). Light source: Xe lamp with 420 nm cutoff filter (3.2 mW).

for semiconductor material was performed using the HEP targeted at bismuth-based binary oxides. We selected target materials from XRD data marked as highly reliable (★) in the Powder Diffraction File[32] because crystal structures marked with a ★ are easily identified and the composition is generally predominant. Table 2 shows the selected target materials as library members and their location printed on the conductive glass substrate. The samples were prepared by mixing the EMOD solutions at the desired composition ratios, printing on the substrate, and firing at 550 °C. The photocurrent was evaluated by application of a potential of −0.1 V (vs Ag/AgCl) for p-type semiconductors and 1.0 V (vs Ag/AgCl) for n-type semiconductors. Under anodic bias, no sample showed a distinct anodic photocurrent. On the other hand, under cathodic bias, a remarkable cathodic photocurrent was observed in the sample targeted for $CuBi_2O_4$ (Figure 10).

From the XRD measurement, the oxide film showed the pattern of tetragonal type $CuBi_2O_4$ (Figure 11). A porous structure was confirmed in SEM observation. The $CuBi_2O_4$ particles were 15−30 nm in diameter, and the aggregated particles were 100-400 nm. Figure 12 shows the current−potential properties of the $CuBi_2O_4$ film under ultraviolet and visible light (without filter) and visible light (420 nm cutoff filter in use) in DEP. A relatively high photocurrent was observed under ultraviolet and visible-light conditions. Under visible-light conditions, the $CuBi_2O_4$ film also showed a high photocurrent that was more than half that under ultraviolet and visible-light conditions. Therefore, we conclude that $CuBi_2O_4$ has high visible-light responsiveness. The $CuBi_2O_4$ was dark brown, and its threshold of absorption was approximately 800 nm. Furthermore, the passage of

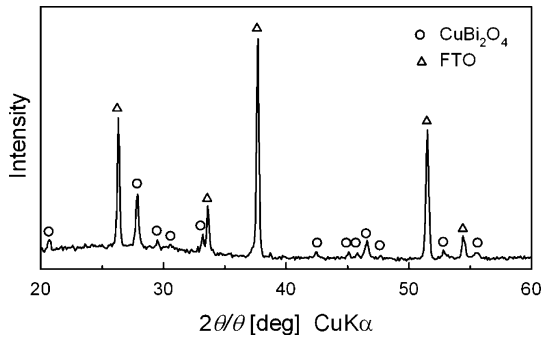

Figure 11. XRD profile of the sample prepared for $CuBi_2O_4$ as the targeted material using the DEP.

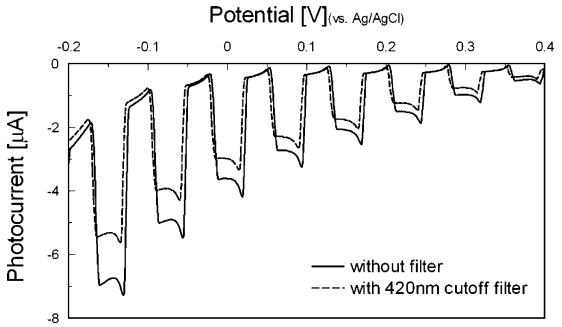

Figure 12. Current−potential curve of the $CuBi_2O_4$ film electrode. The photoelectrode was prepared by painting and firing at 550 °C for 30 min, one time, using DEP. Electrolyte: 0.1 M Na_2SO_4 aqueous solution (pH 5.8). Light source: Xe lamp (9 mW without filter).

photoelectrons (Coulomb number) for 2 h was about 0.026 C (0.27 μmol), whereas the amount of $CuBi_2O_4$ under irradiation was about 0.02 μmol. Therefore, from the results of the current−time measurement the turnover number of the observed photoelectrons to the unit of $CuBi_2O_4$ was approximately 13 for 2 h. This material was confirmed to be stable as a photoelectrode. As mentioned above, $CuBi_2O_4$ was found as a new visible-light-responsive p-type semiconductor using our high-throughput screening system.

4. Summary

The development of a high-throughput screening system is needed for the expeditious discovery of new visible-light-responsive semiconductor materials for photoelectrodes and photocatalysts. For this study, we selected photoelectrochemical measurement for the speedy and convenient evaluation of the visible-light responsiveness of materials, and we developed an automated synthesis system and a high-speed evaluation system for photoelectrodes. For the synthesis, a wet process such as the metal organic decomposition (MOD) method was selected because of its high versatility. This method is also suitable to synthesize the porous film photoelectrode. For the evaluation, the HEP and DEP are used to make the screening process efficient for an enormous number of samples.

As examples of the application of this system, various experiments were performed. In the screening of iron-based binary oxides, an improvement of photocurrent compared with iron oxide was observed in the Fe−Ti and Fe−Nb systems, which showed good consistency with previous reports. These examples show the capability of this system. In the Fe−V system, an improvement of the photocurrent was observed for the composition ratio corresponding with $FeVO_4$. This material is expected to be a new promising n-type semiconductor with high efficiency under visible light. As a result of the screening for p-type semiconductors targeted at bismuth-based binary oxides, $CuBi_2O_4$ was found to be a new material with high visible-light responsiveness. The system made it possible to obtain the above results speedily and easily. We expect that our system will speed up the research progress in the fields of photoelectrodes and photocatalysts.

Acknowledgment. This study was supported by the New Energy and Industrial Technology Development Organization (NEDO) of Japan.

Supporting Information Available. Screening data for the iron-based binary oxide and the reproducibility of the sample. This material is available free of charge via the Internet at http://pubs.acs.org.

References and Notes

(1) Fujishima, A.; Honda, K. *Nature* **1972**, *238*, 37.
(2) Fujishima, A.; Hashimoto, K.; Watanabe, T. *TiO_2 Photocatalysis Fundamentals and Applications*; BKC: Tokyo 1999.
(3) Zou, Z.; Ye, J.; Sayama, K.; Arakawa, H. *Nature* **2001**, *414*, 625.
(4) Domen, K.; Kondo, J. N.; Hara, M.; Takata, T. *Bull. Chem. Soc. Jpn.* **2000**, *73*, 1307−1331.
(5) Kato, H.; Kudo, A. *J. Phys. Chem. B* **2002**, *106*, 5029−5034.
(6) Kudo, A.; Ueda, K.; Kato, H.; Mikami, I. *Catal. Lett.* **1998**, *53*, 229−230.
(7) Santato, C.; Ulmann, M.; Augustynski, J. *J. Phys. Chem. B* **2001**, *105*, 936.
(8) Sayama, K.; Nomura, A.; Zou, Z.; Abe, R.; Abe, Y.; Arakawa, H. *Chem. Commun.* **2003**, 2908−2909.
(9) Aroutiounian, V. M.; Arakelyan, V. M.; Shahnazaryan, G. E. *Sol. Energy* **2005**, *78*, 581−592.
(10) Sartoretti, C. J.; Alexander, B. D.; Solarska, R.; Rutkowska, I. A.; Augustynski, J. *J. Phys. Chem. B* **2005**, *109*, 13685−13692.
(11) Solarska, R.; Alexander, B. D.; Augustynski, J. *C. R. Chim.* **2006**, *9*, 301−306.
(12) Miyake, H.; Kozuka, H. *J. Phys. Chem. B* **2005**, *109*, 17951−17956.
(13) Lettmann, C.; Hinrichs, H.; Maier, W. F. *Angew. Chem., Int. Ed.* **2001**, *40*, 3160−3164.
(14) Dai, Q. X.; Xiao, H. Y.; Li, W. S.; Na, Y. Q.; Zhou, X. P. *J. Comb. Chem.* **2005**, *7*, 539−545.
(15) Kim, H. G.; Borse, P. H.; Choi, W.; Lee, J. S. *Angew. Chem., Int. Ed.* **2005**, *44*, 4585−4589.
(16) Bessekhouad, Y.; Robert, D.; Weber, J.-V. *Catal. Today* **2005**, *101*, 315−321.
(17) Long, M.; Cai, W.; Cai, J.; Zhou, B.; Chai, X.; Wu, Y. *J. Phys. Chem. B* **2006**, *110*, 20211−20216.
(18) Siripala, W.; Ivanovskaya, A.; Jaramillo, T. F.; Baeck, S-H.; McFarland, E. W. *Sol. Energy Mater. Sol. Cells* **2003**, *77*, 229−237.
(19) Miller, E. L.; Paluselli, D.; Marsen, B.; Rocheleau, R. E. *Sol. Energy Mater. Sol. Cells* **2005**, *88*, 131−144.
(20) Turner, J. E.; Hendewerk, M.; Parmeter, J.; Neiman, D.; Somorjai, G. A. *J. Electrochem. Soc.* **1984**, *131*, 1777−1783.
(21) Matsumoto, Y.; Omae, M.; Sugiyama, K.; Sato, E. *J. Phys. Chem.* **1987**, *91*, 577−581.

(22) Aroutiounian, V. M.; Arakelyan, V. M.; Shahnazaryan, G. E.; Stepanyan, G. M.; Turner, J. A.; Khaselev, O. *Int. J. Hydrogen Energy* **2002**, *27*, 33−38.
(23) Jaramillo, T. R.; Baeck, S-H.; Kleiman-Shwarsctein, A.; Choi, K-S.; Stucky, G. D.; McFarland, E. W. *J. Comb. Chem.* **2005**, *7*, 264−271.
(24) Woodhouse, M.; Herman, G. S.; Parkinson, B. A. *Chem. Mater.* **2005**, *17*, 4318−4324.
(25) Funahashi, R.; Urata, S.; Kitawaki, M. *Appl. Surf. Sci.* **2004**, *223*, 44−48.
(26) Please see the Supporting Information.
(27) Please see the Supporting Information for some screening data on the Fe binary oxide.
(28) Kudo, A.; Hijii, S. *Chem. Lett.* **1999**, 1103−1104.
(29) Tang, J.; Zou, Z.; Ye, J. *Angew. Chem., Int. Ed.* **2004**, *43*, 4463−4466.
(30) Zou, Z.; Ye, J.; Sayama, K.; Arakawa, H. *Chem. Phys. Lett.* **2001**, *343*, 303−308.
(31) Kim, H. G.; Hwang, D. W.; Lee, J. S. *J. Am. Chem. Soc.* **2004**, *126*, 8912−8913.
(32) Alphabetical Indexes Inorganic Phases Sets 1−48. *Powder Diffraction File*; McClune, W. F., Ed.; JCPDS-International Center for Diffraction Data: Newtown Square, PA, 1998.

CC0700142